Int. J. Solids Structures Vol. 17, pp. 769-785, 1981
Printed in Great Britain.

0020-7683/81/080769-17$02.00/0

MOTION OF RIGID SPHERES THROUGH ELASTIC TUBES

AYDIN TÖZEREN
Deparmment of Engineering Sciences, Middle East Technical University, Ankara, Turkey

(*Received* 13 *June* 1980; *in revised form* 27 *October* 1980)

Abstract—The steady motion of a line of rigid spherical particles in a thin elastic shell of smaller diameter is considered Coulomb's law of friction is assumed to hold on the contact surface between the spheres and the shell. The case in which the particle radius is comparable to the inner shell radius is investigated by using small deformation elastic shell theory. Furthermore, the case in which the diameter ratio is large is considered by neglecting the bending stiffness of the shell. Equations of motion are reduced to a set of nonlinear differential equations. An iterative procedure is introduced to determine the location of free boundaries seperating the contact region from rest of the shell. The force required to pull the sphere with constant speed is calculated as a function of the elastic properties of the shell, coefficient of friction on the contact surface, the diameter ratio and the speed V_0 of the spherical particles.

1. INTRODUCTION

Uniaxial motion of a line of particles in a rigid tube filled with fiuid was extensively studied by many authors (See [1] for references). Tözeren and Skalak [1] considered the flow of an elastic sphere in a tube of smaller inner diameter. They introduced an iterative procedure to combine lubrication analysis with a series solution giving the displacement field of an elastic sphere moving in a rigid tube of comparable diameter. A variational principle was introduced and finite element analysis was employed by Zarda *et al.* [2] to study the motion of highly deformable cells in rigid tubes.

The motion of uniform plastic shell has also been extensively considered [3]. However non-linear analysis corresponding to large deformations was mainly restricted to stability and vibrations of shells undergoing radial deflections [4].

Contrary to the articles mentioned above in which particles are assumed deformable and the tube rigid, this paper investigates the steady motion of a line of rigid spherical particles in a thin elastic shell of smaller diameter. The impetus for undertaking this problem comes from the studies of the mechanical behavior of ureters obstructed by calculi and motion of white blood cells in narrow capillary blood vessels. However, the analysis may be relevant for a wide class of problems involving particle-vessel interactions. In such cases the present treatment may serve as a starting point or qualitative guide to the nature of results to be expected.

Coulomb's law of friction is assumed to hold on the contact surface between the sphere and the shell. The location of the boundary seperating part of the inner shell from the part still in contact to the surface of the sphere is not known in advance, but will be found as part of the solution. Present study constitutes an example of a free boundary problem. Burridge and Keller [5] considered several cases of peeling, slipping and cracking involving a one dimensional continuum with a free boundary. Such problems may be intrinsically of interest to the research fields of crack formation, fault plane slippage and rouleaux formation of red blood cells.

The force required to move a sphere with constant speed through a circular cylindirical shell depends strongly on the ratio of the particle diameter to the inner shell diameter ($\lambda = R_0/a$). If this ratio is slightly greater than one, bending moment M_1 and the shear force Q_1 are major unknown quantities in the analysis. This case is treated first. Infinitesimal deflections on the shell middle surface and pressure distribution on the contact region are calculated using the assumptions of linear elastic shell theory.

Bending stiffness of the shell is not important in severe deformations that occur when diameter ratio λ is large. The thin shell then can be studied as a membrane tube. The analysis of the shell in this case will be carried out for two different hyperelastic materials. Equilibrium equations are reduced to a set of non-linear differential equations.

An iterative procedure is introduced to determine the location of the free boundary and to combine the solutions obtained for the contact region and the free part of the shell. The force required to pull the sphere with constant speed is calculated as a function of λ, coefficient of friction, μ and the elastic properties of the shell.

Kinematics of the middle surface of the shell caused by the moving sphere is considered next. Velocity and acceleration vectors are expressed in terms of extension ratios λ_1, λ_2 and their spatial derivatives. Acceleration terms are incorparated into equations of motion. The solution of these equations illustrate the effect of sphere velocity on the deformation of the shell.

Numerical results are presented which illustrate the character of shell deformation for a wide range of the paremeters mentioned above.

2. SHELL EQUILIBRIUM EQUATIONS

Consider a rigid spherical particle of radius R_0 moving axisymmetrically through a circular cylindirical tube with a uniform velocity V_0. The tube is assumed to be a thin elastic shell of uniform initial thickness h_0. The radius R_0 of the sphere is supposed to be greater than the initial inner radius a of the shell. One edge of the shell is fixed in radial and axial directions and the other edge is free as shown in Fig. 1. In the region where sphere touches the shell, the middle surface deforms into a spherical surface with radius $(R_0 + h/2)$, where h denotes the deformed thickness. The boundary of the contact surface is not prescribed, but must be found as part of the solution of the problem. This boundary consists of two circular sections seperating the sphere surface from the inner surface of the shell. These sections are denoted as A and B, section A being the boundary on the side of the free edge as shown in Fig. 1.

Coulomb's law of friction is assumed to hold on the contact surface. The axisymmetric deflections of the shell and the force required to pull the sphere with constant speed is to be determined.

Cylindirical coordinate system (r, θ, z) fixed to the center of the sphere is introduced. The arc length along a meridian reasured from a fixed material point is denoted by s and $\mathring{s}$, respectively in the deformed and undeformed positions. Due to the symmetry of deformation, principal directions of strain at any point coincide with the meridional, circumferential and normal directions at the same location on the middle surface.

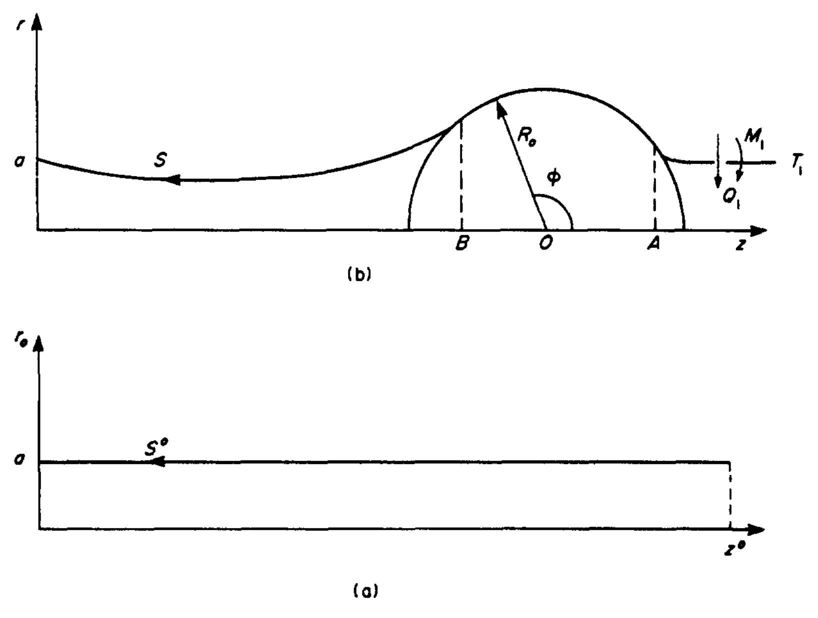

Fig. 1. Inital and deformed configurations of the elastic shell and sign convention of the resultant forces and moments.

Principal stretch ratios λ_1, λ_2 and λ_3 in these dieections are defined respectively as

$$\lambda_1 = \frac{ds}{ds_0}, \quad \lambda_2 = \frac{r}{a}, \quad \lambda_3 = \frac{h}{h_0} \tag{1}$$

where r denotes the radial distance from the z axis of the cylindirical shell. For tubes of incompressible material stretch ratio $\lambda_3 = 1/(\lambda_1\lambda_2)$.

The angle that the normal to the middle surface makes with the axial direction is denoted by ϕ and is shown in Fig. 1. The principal curvatures k_1 and k_2 are defined by relations.

$$k_1 = (d\phi/ds), \quad k_2 = \sin\phi/r. \tag{2}$$

It is assumed that lines perpendicular to the middle surface before deformation remain perpendicular after deformation. Stress resultants of the shown in Fig. 2. Equations of motion for a thin shell are, from Timoshenko and Kreiger[6],

$$\frac{dT_1}{ds} + \frac{1}{r}\frac{dr}{ds}(T_1 - T_2) - k_1 Q_1 + P_1 = \rho a_t \tag{3}$$

$$k_1 T_1 + k_2 T_2 + \frac{1}{r}\frac{d}{ds}(rQ_1) - P_3 = -\rho a_n \tag{4}$$

where

$$Q_1 = \frac{1}{r}\frac{dr}{ds}(M_2 - M_1) - \frac{dM_1}{ds}. \tag{5}$$

M_1 and M_2 are the bending moments per unit of final length in the meridional and circumferential directions respectively and Q_1 is the shear force per unit of final length perpendicular to the middle surface. T_1 and T_2 are membrane tensions per unit of final length and P_1 and P_3 are the tangential and normal loads per unit of final area, respectively. Contact forces are supposed to apply on the middle surface of the shell. Components of acceleration vector along the tangential and normal directions are denoted by a_t and a_n, respectively. Note that areal density ρ in eqns (3) and (4) are related to the constant density ρ_0 of the shell by the equation

$$\rho = \lambda_3 h_0 \rho_0. \tag{6}$$

If the radius R_0 of the sphere is only slightly greater than the inner radius of the tube, shell equations can be based on the assumptions of linear theory of elasticity. As a starting point, this solution will be outlined in the next section before analysing the finite deformations of a hyperelastic shell caused by the large values of λ.

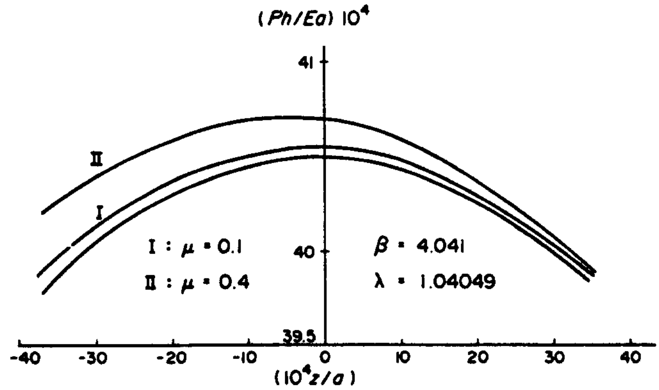

Fig. 2. Variation of Contact pressure with respect to he axis of the tube ($\lambda = 1.04049$, $\mu = 0.1$, $\mu = 0.4$).

3. SMALL STRAIN ANALYSIS

Equilibrium equations for the thin shell under the assumptions of small strain reduce to [6]

$$\frac{dT_1}{dz}+P_1=0 \tag{6}$$

$$\frac{dQ_1}{dz}+\frac{T_2}{a}-P_3=0 \tag{7}$$

where $Q_1=-(dM_1/dz)$. It will be more suitable in this case to describe the deformation, in terms of a displacement vector. Components along the r and z directions are denoted by w and u respectively. Displacement component v in the circumferential direction vanishes. Assuming Hooke's law, stress resultants and bending moments can be expressed in the form:

$$T_1=\frac{Eh}{1-\nu^2}\left(\frac{du}{dz}+\nu\frac{w}{a}\right),\quad T_2=\frac{Eh}{1-\nu^2}\left(\frac{w}{a}+\nu\frac{du}{dz}\right) \tag{8}$$

$$M_1=-D(d^2\,w/d\,z^2),\quad M_2=-\nu D(d^2\,w/d\,z^2) \tag{9}$$

where E denotes the Young's modulus, ν is the Poisson's ratio and D is the flexural rigidity of the shell $(D-Eh^3)/(12(1-v^2))$.

The deformation of the shell depends strongly on the two geometric parameters λ and (h/a). It can be shown that

$$\frac{w}{a}=(\lambda-1)e^{-|\beta z|}(\sin|\beta z|+\cos|\beta z|),\quad \lambda\leq 1+\frac{(h/a)}{2[3(1-\nu^2)]^{1/2}}. \tag{10}$$

The parameter β is defined as $\beta^4=3(1-\nu^2)/(a^2h^2)$. This solution corresponds to the case where the bending rigidity of the shell allows the sphere to touch the inner surface only at a singular arc. For greater values of λ, the contact region becomes a spherical surface and the displacement w on the contact surface can be approximated as:

$$(w/a)=(\lambda-1)-(z/a)^2/2. \tag{11}$$

In this domain, dimensionless displacement (u/a) and pressure (P_3a/Eh) can be shown to be expressed in the form

$$\frac{u}{a}=B_1+B_2e^{-\mu\nu(z/a)}+\frac{z^3}{6\nu a^3}+\frac{(\nu-1)}{2\mu\nu^2}\frac{z^2}{a^2}+\left(\frac{1-\nu^3}{\mu^2\nu^3}-\frac{(\lambda-1)}{v}\right)\frac{z}{a} \tag{12}$$

$$\frac{P_3a}{Eh}=\left(\lambda-1-\frac{1}{\mu^2\nu^2}+\frac{z_A}{\mu\nu a}\right)e^{-\mu\nu(z-z_A)/a}+\frac{1}{\mu^2\nu^2}-\frac{z}{\mu\nu a} \tag{13}$$

where B_1 and B_2 are constrants of integration and μ is the coefficient of friction on the contact surface. In eqn (13) boundary condition at unknown location A

$$P_3(z_A)=T_2(z_A)/a \tag{14}$$

has been employed where z_A denotes the z coordinate of section A. When contact surface is smooth $(\mu=0)r$, pressure distribution is given by the equation

$$(P_3a/Eh)=((\lambda-1)-(z/a)^2/2). \tag{15}$$

The free part of the shell in which there are no external loads is physically divided into two regions by the sphere. In this domain solution of equilibrium equations yields displacement component (w/a) as

$$\frac{w}{a}=\frac{e^{-\beta x^{(\alpha)}}}{2\beta^2a^2}(A_1^{(\alpha)}\sin\beta x^{(\alpha)}+A_2^{(\alpha)}\cos\beta x^{(\alpha)})-\nu\frac{T^{(\alpha)}}{Eh},$$

where

$$x^{(A)} = z - z_A, \quad x^{(B)} = z_B - z, \quad \alpha = A,B. \tag{16}$$

Boundary conditions at infinity

$$\frac{w}{a} = -\frac{\nu T^{(\alpha)}}{Eh}, \quad \frac{\mathrm{d}w}{\mathrm{d}z} = \frac{\mathrm{d}^2 w}{\mathrm{d}z^2} = 0 \text{ as } x^{(\alpha)} \to \infty$$

are already staisfied by eqn (16). In the case of a single sphere moving inside the tube, stress resultant T_1 is equal to zero in the domain $z_A \leq z < \infty$. However there will be a uniform tension $T_1 = T^{(B)}$ along the meridian of the shell in $(-\infty < z \leq z_B)$ given by equation

$$T^{(B)} = \mu \int_{z_B}^{z_A} P_3(z)\,\mathrm{d}z. \tag{17}$$

Tension $T^{(B)}$ depends on locations of A and B, and integrand P_3 is given by eqn (13).

The boundary conditions at A and B can be stated as

$$[w] = \left[\frac{\mathrm{d}w}{\mathrm{d}z}\right] = \left[\frac{\mathrm{d}^2 w}{\mathrm{d}z^2}\right] = 0 \text{ at } z = z_\alpha, \ \alpha = A,B. \tag{18}$$

Here for any function $g(z, t)$, $g(z_\alpha', t)$ is the limit of $g(z, t)$ as z approaches z_α from above and below, and

$$[g(z_\alpha, t)] = g(z_\alpha^+, t) - g(z_\alpha^-, t).$$

Comparison of eqns (11) and (16) show that these continuity requirements are satisfied if

$$A_1^{(\alpha)} = 1, \quad A_2^{(\alpha)} = \left[8\beta^2 a^2\left(\lambda - 1 + \frac{\nu}{Eh} T^{(\alpha)}\right)\right]^{1/2} - 1 \tag{19a}$$

$$\frac{z_\alpha}{a} = (A_2^{(\alpha)} - 1)/2\beta a. \tag{19b}$$

A simple iterative procedure is needed to determine the values of $A_2^{(B)}$, z_B, and $T^{(B)}$ from eqns (17), (19*a* and 19*b*). The computational cycle is repeated until the additional tension $\Delta T^{(B)}$ becomes sufficiently small.

The dimensionless force required to pull the sphere $(F_z/2\pi ahE)$ is equal to $(T^{(B)}h/aE)$ when the region of contact between the sphere and the shell is a surface. For values of λ such that the contact is along a circular arc

$$\frac{F_z}{2\pi ahI} = \frac{2\mu}{[3(1-\nu^2)]^{1/4}}(\lambda - 1)(h/a)^{1/2}. \tag{20a}$$

It is expedient to present numerical results in terms of dimensionless variables. Elasticity parameter $(a\beta)$, coefficient of friction. μ and diameter ratio λ are chosen as independent parameters. Computations are carried out for values of $(a\beta)$ such that ratios (h/a) and $(\lambda - 1)$ remains in the same order of magnitude. Numerical results using eqns (12) and (14) indicate that effect of frictional forces on the pressure distribution P_3 is negligible (Fig. 2). For contact problems involving small strains of elastic continuum, this fact is generalized as a widely used assumption to obtain solutions for the contact pressure P_3[8]. Using the pressure distribution for $\mu = 0$ as an approximation, the force required to pull the sphere can be expressed as

$$\frac{F_z}{2\pi ahE} = 2\mu\left[\frac{\sqrt{2}}{6}(\lambda - 1)^{3/2} + \frac{5(\lambda - 1)(h/a)^{1/2}}{3[3(1-\nu^2)]^{1/4}} - \frac{\sqrt{(2)}(\lambda - 1)^{1/2}(h/a)}{2[3(1-\nu^2)]^{1/2}}\right. \tag{20b}$$

$$\left. + \frac{(h/a)^{3/2}}{6[3(1-\nu^2)]^{3/4}}, \quad \lambda \geq 1 + \frac{(h/a)}{2[3(1-\nu^2)]^{1/2}}.\right.$$

F_z increases linearly with μ. Figure 4 shows the dimensionless force $(F_z/2\pi ahE)$ plotted against $(\lambda - 1)$ for a set of values of (h/a).

Combination of the solutions obtained above shows that bending moment M_1 is equal to (D/a) at the contact surface and is continuous at boundaries A and B. However shear force Q_1 will have a finite jump from its zero value on the contact surface to values $Q^{(a)} = D(1 + A_2^{(a)}/a)$ at boundaries A and B. The distributions of dimensionless displacement (w/a), bending moment (aM_1/D) and the shear force (a^2Q_1/D) along the axis of the shell are illustrated in Fig. 3. Results indicate that solutions approach asymptotically to zero at either direction effectively within a

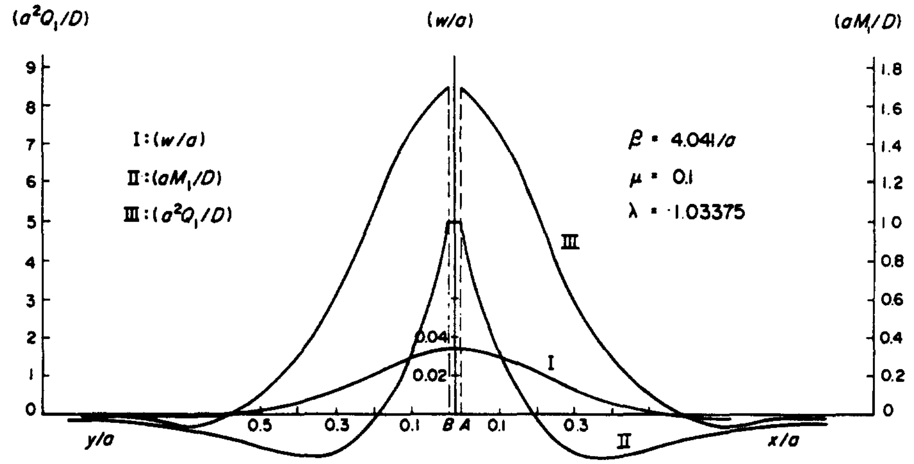

Fig. 3. Variations of radial displacement w_1 resultant moment M_1 and resultant shear Q_1 along the axis of the shell ($\lambda = 1.03375$, $\beta = 4.041$, $\mu = 0.1$).

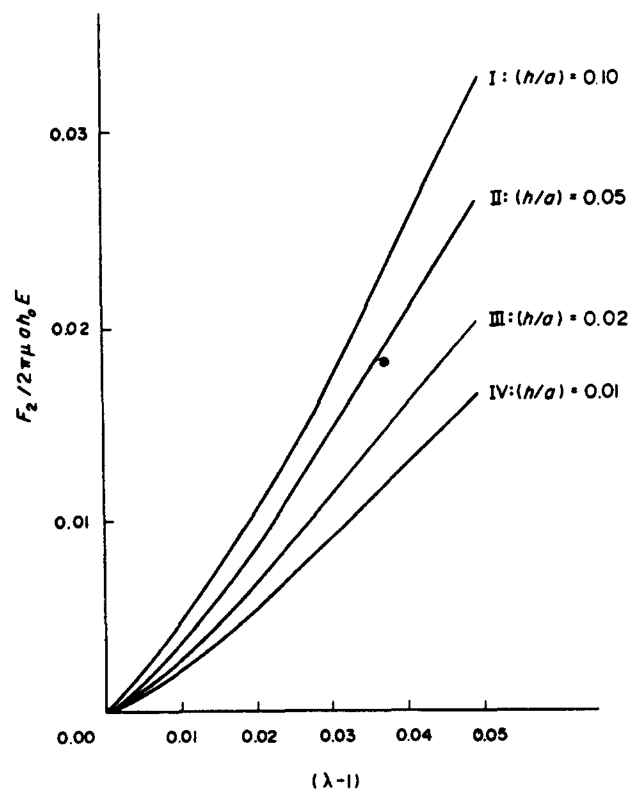

Fig. 4. Force required to pull the sphere with constant speed in a tube of slightly smaller diameter as a function of λ.

distance that equals to the radius of the sphere. This indicates that the solutions described in section three can easily be generalized for a line of spherical particles even when the particle spacing is taken to be equal to one particle diameter $2R_0$.

4. MEMBRANE ANALYSIS OF THE SHELL

In this section, severe deformations of the thin shell caused by large values of diameter ratio λ will be considered. In this cause, tensions T_1 and T_2 play a dominant role; bending moments M_1, M_2 and shear resultant Q_1 are neglected in equations of equilibrium. The thin shell is assumed to either made of Mooney material or a biological membrane described by Skalak *et al.*[9].

The stress resultants T_1 and T_2 for an incompressible Mooney material can be expressed in the form

$$T_1 = 4h_0C_1\lambda_3(\lambda_1^2 - \lambda_3^2)(1 + \Gamma\lambda_2^2) \tag{21}$$

$$T_2 = 4h_0C_1\lambda_3(\lambda_2^2 - \lambda_3^2)(1 + \Gamma\lambda_1^2) \tag{22}$$

where C_1 and Γ are constants and $\lambda_3 = 1/\lambda_1\lambda_2$.

Another case that will be studied is the shell made of a biological membrane that strongly resists any attempt to change it's surface area but is easily deformed at constant area. The constitutive equations for a hyper-elastic material that has this property is given as[8]

$$T_1 = -p + \frac{B}{2}\lambda_1^2(\lambda^2 - 1) \tag{23}$$

$$T_2 = -p + \frac{B}{2}\lambda_2^2(\lambda_2^2 - 1) \tag{24}$$

where B is a material constant, $-p$ is the isotropic tension and $\lambda_1 = 1/\lambda_2$ required by the constant area condition. Since the material is assumed to be incompressible, the thickness h_0 of the shell do not change with deformation.

The cylindirical middle surface will deform in to a spherical surface with radius R_0 in the contact region bounded by sections A and B. Equations of equilibrium in normal and tangential directions reduce to

$$T_1 + T_2 = R_0P_3 \tag{25}$$

$$\frac{dT_1}{d\phi} = \cot\phi(T_2 - T_1) + \mu(T_1 + T_2) \tag{26}$$

where polar angle ϕ is considered as the independent variable. External load P_1 was eliminated in eqns (25) and (26) by using Coulomb's law of friction. The boundary A is located with respect to the center of the sphere at $\phi_A = \sin^{-1}(a/R_0)$ since the bending stiffness of the shell is neglected. At this location boundary condition can be stated as

$$T_1(\phi_A) = T_2(\phi_A) = 0. \tag{27}$$

Extension ratio λ_2 on the spherical contact surface is given in the form

$$\lambda_2 = (R_0/a)\sin\phi. \tag{28}$$

A first order differential equation is obtained for principle extension λ_1 if eqns (21) and (22) of tensions T_1, T_2 of Mooney material are substituted into eqn (26)

$$\begin{aligned}\frac{d\lambda_1}{d\phi} = [&\cot\phi\,(\lambda_2^2(1 - \lambda_1^2\Gamma) - \lambda_2^{-2}(\Gamma + 3\lambda_1^{-2})) + \\ &+ \mu(2\Gamma(\lambda_1^2\lambda_2^2 - \lambda_1^{-2}\lambda_2^{-2}) + \lambda_1^2 + \lambda_2^2 - \Gamma(\lambda_1^{-2} + \lambda_2^{-2}))]/ \\ &[\lambda_1(1 + \Gamma\lambda_2^2)(1 + 3\lambda_1^{-2}\lambda_2^{-2})]\end{aligned} \tag{29}$$

where λ_2 is given by eqn (28). Numerical integration of (29) satisfying condition (27) at A reveals the distribution of λ_1 on the contact surface. Tensions T_1, T_2 and pressure P_3 are obtained by using eqns (21), (22) and (25), respectively.

Pressure distribution on the contact surface of Mooney shell assuming $\mu = 0$ is shown in Fig. 5(a) for increasing values of parameter λ. It will be observed in this case that an initial rise in inflating pressure will be followed by a fall as diameter ratio $\lambda = (R_0/a)$ increases. This is similar to the softening phenomenon is readily observed during the inflation of a spherical rubber balloon[10]. The variation of pressure distribution P_3 with coefficient of friction μ is illustrated in Fig. 5(b). As can be seen from this graph effect of tangential contact stress on pressure P_3 can not be neglected in large deformations of the shell.

Extension ratio λ_1 of biological membrane is equal to $(1/\lambda_2)$ in this region due to constant

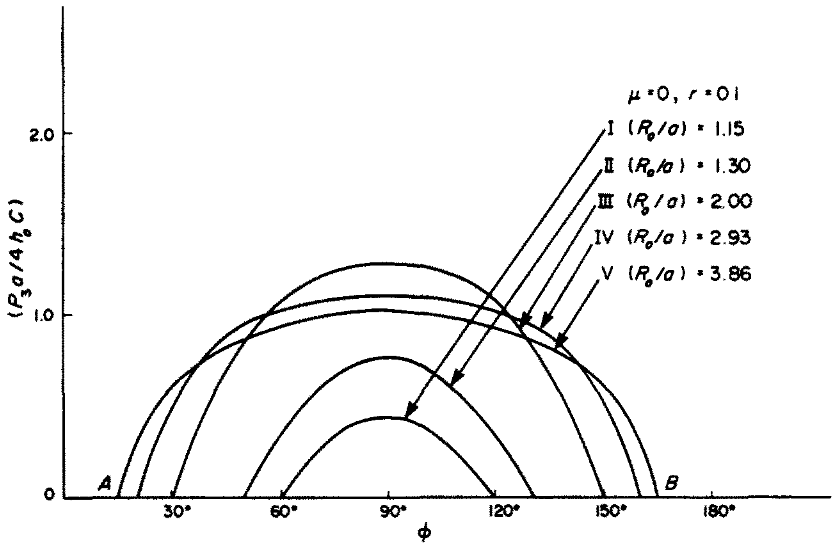

(a)

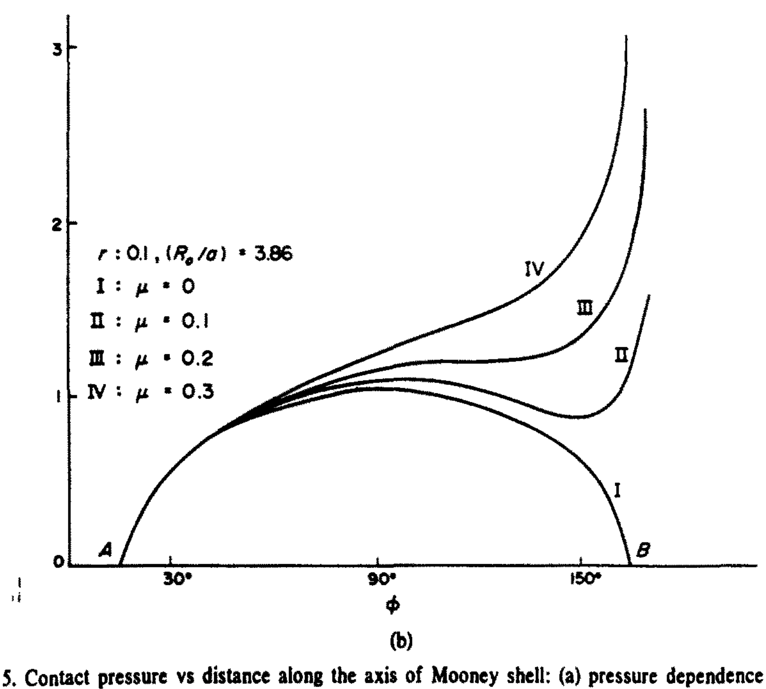

(b)

Fig. 5. Contact pressure vs distance along the axis of Mooney shell: (a) pressure dependence on λ; (b) pressure dependence on μ.

surface area stipulation. A differential equation for pressure P_3 is obtained by eliminating isotropic stress $(-p)$ from eqns (25) and (26)

$$\frac{dP_3}{d\phi}-2\mu P_3=-\frac{B}{2}\cos\phi[-6\lambda^3\sin^3\phi+4\lambda\sin\phi-2\lambda^{-5}\sin^{-5}\phi]. \quad (30)$$

The solution of (30) satisfying condition (27) can be written in the form:

$$(2P_3a/B)=e^{2\mu\phi}\left[\int_{\phi_A}^{\phi}e^{-2\mu\phi}\cos\phi(6\lambda^3\sin\phi^3-4\lambda\sin\phi+2\lambda^{-5}\sin^{-5}\phi)d\phi\right]. \quad (31)$$

Variation of this pressure distribution with respect to parameters λ and μ are shown in Fig. 6(a) and Fig. 6(b), respectively. As can be seen from these figures the contact pressure increases with increasing λ contrary to the softening behavior of Mooney shell. However the effect of μ on the contact pressure is very similar in both types of tubes, increasing rhe pressure in the domain $z_B<z<0$ (Fig. 6b).

Stress resultants T_1 and T_2 and isotropic tension $(-p)$ are obtained by substituting (31) into eqns (23)–(25) respectively.

The force required to move the sphere inside the tube with constant speed V_0 may be expressed as

$$F_z=2\pi R_0^2\int_{\phi_A}^{\phi_B}(P_3\cos\phi+\mu P_3\sin\phi)\sin\phi\, d\,\phi. \quad (32)$$

In order to estimate this force the location of free boundary B must be determined. The boundary conditions at B can be states as

$$[T_1(z_B)]=[T_2(z_B)]=\left[\frac{dT_1}{dz}\right]=\left[\frac{dT_2}{dz}\right]=0 \text{at } z=z_B \quad (33)$$

which requires the continuity of λ_1, λ_2, $(-p)$ and their first spatial derivatives.

In free part of the shell $(-\infty<z<z_B)$ equilibrium equations in tangential and normal directions can be reduced to

$$\frac{dT_1}{d\lambda_2}=\frac{1}{\lambda_2}(T_2-T_1) \quad (34)$$

$$\frac{a^2(d^2\lambda_2/dz^2)}{[1+a^2(d\lambda_2/dz)^2]}=\frac{T_2}{\lambda_2T_1}. \quad (35)$$

If constitutive equations for tensions T_1, T_2 are substituted into eqn (34), the resulting differential equation can be integrated with respect to λ_2. In the case of biological membrane T_1 is obtained in the form

$$T_1=D_1+\frac{B}{2}[(\lambda_2^4/4)+(\lambda_2^{-4}/4)-(\lambda_2^2/2)-(\lambda_2^{-2}/2)] \quad (36)$$

where

$$D_1=T_1^B-\frac{B}{2}[(\lambda_2^B)^4/4+(\lambda_2^B)^{-4}/4-(\lambda_2^B)^2/2-(\lambda_2^B)^{-2}/2] \quad (37)$$

is constant of integration determined by the requirement that T_1 be continous at section B. The symbol λ_2^B denotes the value of λ_2 computed by using the solution valid in the spherical contact region at unknown location $\phi=\phi_B$.

Tension T_2 can similarly be written as a function of single variable λ_2 by eliminating $(-p)$ in eqns (23) and (24) and using the relation $\lambda_1=1/\lambda_2$.

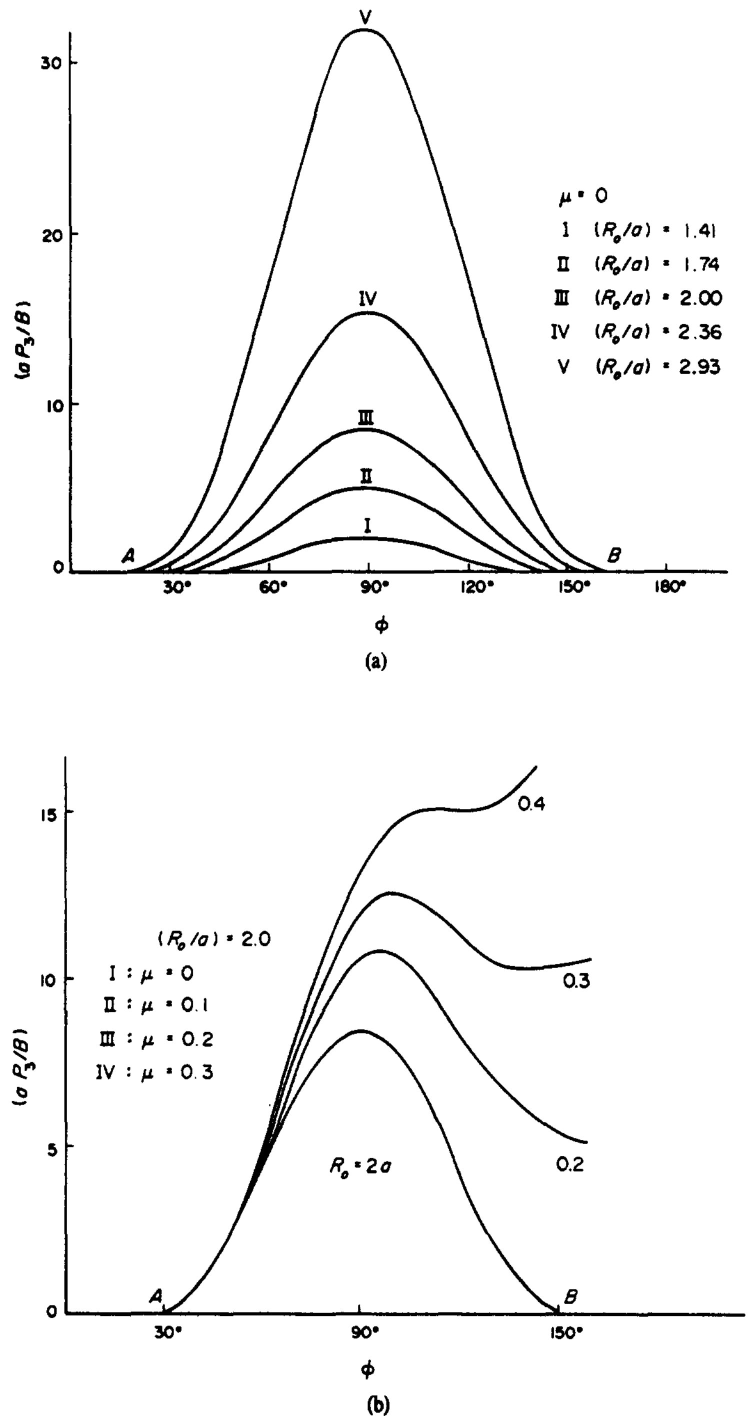

Fig. 6. Contact pressure vs distance along the axis of biological shell: (a) pressure dependence on λ; (b) pressure dependence on μ.

If the shell is made of Mooney material eqn (34) is reduced, after suitable manipulations, to a differential equation in the form

$$(\Gamma+3\lambda_1^4\lambda_2^4)[d(\lambda_1^4\lambda_2^2)/dz] = d(\lambda_2^2)/dz - d(\lambda_1^2)/dz - (\Gamma/\lambda_2^4)(d(\lambda_2^2)/dz) - (3\Gamma/\kappa_1^4)(d(\lambda_1^2)/dz). \quad (38)$$

The integration of this equation with respect to z reveals the relation

$$(\Gamma\lambda_2^2+1)\lambda_1^4 - (\lambda_2^2+\Gamma/\lambda_2^2+D_2)\lambda_1^2 - 3/\lambda_2^2 - 3\Gamma = 0 \quad (39)$$

where integration constant D_2 is found by the requirement that T_1, T_2 be continous at B

$$D_2 = \Gamma(\lambda_2{}^B\lambda_1{}^B)^2 - 3(\lambda_1{}^B\lambda_2{}^B)^{-2} - (\lambda_2{}^B)^2 + (\lambda_1{}^B)^2 - \Gamma((\lambda_2{}^B)^{-2} - 3(\lambda_1{}^B)^{-2}). \tag{40}$$

Extension ratio λ_1 is obtained as a function of λ_2 by using the positive root of this polynomial for $\lambda_1{}^2$. Tensions T_1 and T_2 are then found by using eqns (21) and (22).

In order to complete the analysis of deformation, extension ratio λ_2 must be expressed as a function of z. A new dependent variable q defined by the relation

$$q = a^2(\mathrm{d}\lambda_2/\mathrm{d}z)^2 \tag{41}$$

is introduced in to the second order differential equation (35). After integration with respect to λ_2, the solution that satisfies the conditions (33) is written in the form:

$$1 + a^2(\mathrm{d}\lambda_2/\mathrm{d}z)^2 = (1 + \lambda^2 \cos \phi_B{}^2) \exp\left[2\int_{\lambda_2{}^B}^{\lambda_2} (T_2/(\lambda_2 T_1))\mathrm{d}\lambda_2\right]. \tag{42}$$

Numerical results may be obtained by selecting a suitable value for ϕ_B. Extension ratio λ_2 is found by numerical integration of eqn (42). The location of the fixed edge will be at the section where $\lambda_2 = 1$. If in the domain $(-\infty < z < z_B)$ λ_2 is not equal to one at any point, then this solution will be disregarded. The value of ϕ_B is then increased by increment $\Delta\phi_B$ and the computations are repeated. Force required to pull the sphere is calculated as a function of its distance from the fixed edge of the shell.

In the case of a single spherical particle that is sufficiently distant from the fixed edge of the shell, the location ϕ_B of free boundary B will not change with respect to the center of the particle. The deformation of the shell will be confined to the increase of length of the portion with minimum $\lambda_2 = \lambda_{2m}$. In order to obtain this steady state solution, it will be assumed that

$$(\mathrm{d}\lambda_2/\mathrm{d}z) = (\mathrm{d}^2)_2/\mathrm{d}z^2) = T_2 = 0 \text{ at } \lambda_2 = \lambda_{2m}. \tag{43}$$

Equilibrium eqn (35) is automatically satisfied at $\lambda_2 = \lambda_{2m}$ with this assumption. Integration constants D_1 and D_2 for the biological shell and Mooney shell, respectively, can be written as:

$$D_1 = \frac{B}{2}[-1.25\lambda_{2M}^4 + 0.75\lambda_{2M}^{-4} + 1.5\lambda_{2M}^2 - 0.5\lambda_{2M}^{-2}] \tag{44}$$

$$D_2 = -3\Gamma\lambda_{2m}^4 - 4\lambda_{2m}^2 + \lambda_{2m}^{-4}. \tag{45}$$

Numerical integration of eqn (42) will reveal the solution as a function of z. The polar angle ϕ and the normal distance R are obtained along the axis of the shell by using the relations

$$\phi = \cot^{-1}(a\mathrm{d}\lambda_2/\mathrm{d}z) \tag{46}$$

$$R = a\lambda_2/\sin\phi. \tag{47}$$

Let us denote the tension T_1 obtained from the solution mentioned above valid in the range $(-\infty < z \leq z_B)$ by superscript f. An iterative procedure is established by increasing the value of λ_{2m} by an increment $\Delta\lambda_{2m}$. The free boundary B will be at the location where the conditions

$$T_1{}^c(\phi) = T_{1j}^f(\phi), \; (R/a)^f = (R_0/a)^c \tag{48}$$

are satisfied. Subscript j refers to the solution of jth iteration, and superscript c denotes the solution valid in the contact region.

Numerical computations described above are employed for both types of membrane tubes. Deflected shapes of the elastic shells are illustrated in Fig. 7 for $\lambda = 2$ and a set of μ values. As either one of parameters λ and μ increases, the inner radius of the biological shell decreases

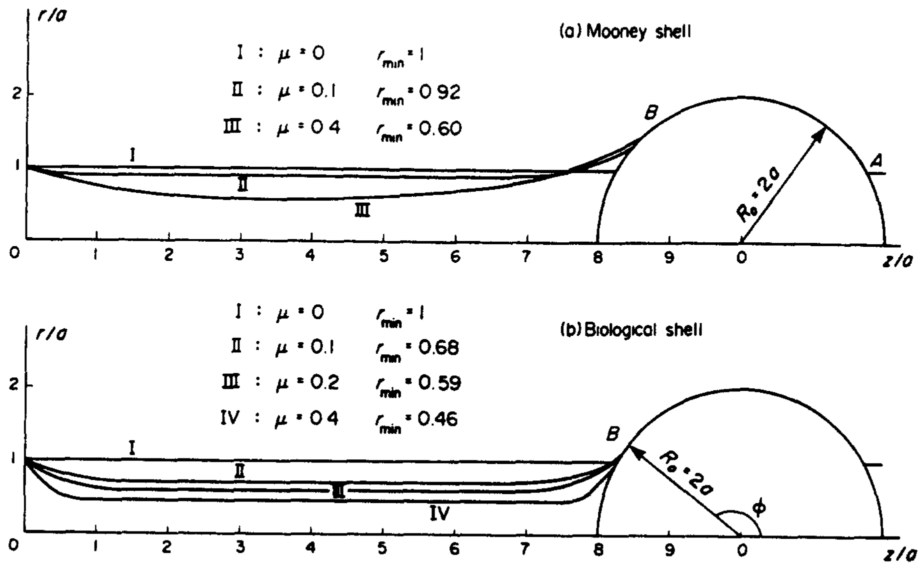

Fig. 7. Finite deformations of elastic shell caused by the motion of the sphere: (a) Mooney shell; (b) biological shell.

rapidly while for the Mooney shell the thickness of the tube becomes thinner to accomodate the motion of the sphere. These two types of behavior would give quite different mechanical results for example if the tube was filled with fluid.

The force required to pull the sphere with constant speed is strongly dependent on the diameter ratio λ. This dependence is illustrated in Fig. 8 for biological shell and Mooney shell. Coefficient of friction μ is employed as a parameter in these figures.

The steady flow of incompressible elastic spheres in a rigid tube of slightly smaller diameter and filled with fluid was considered by [3]. Relative apparent viscosity that represents the pressure drop along the axis of the shell was shown similarly to increase with λ. However, in the region where there is a thin lubrication layer between the shell and the sphere, tangential stresses become negligible and the pressure distribution has only point symmetry with respect to the center of the sphere.

In the case of a line of spherical particles that are sufficiently distant from each other, the analysis will be the same as described above except that the angle ϕ_A will be taken equal to $(\pi - \phi_B^{(n-1)})$ where n denotes the nth sphere further away from the free edge of the shell. Deflected shapes of the elastic shells of biological membrane and Mooney membrane are illustrated in Fig. 9. The force required to pull an additional sphere remains approximately constant in the range of numerical computations that considered at most threee spheres moving in the shell.

5. CONSIDERATION OF INERTIAL EFFECTS

In this section kinematics of deformation of the thin shell will be considered. Acceleration vector will be expressed as a function of extension ratios λ_1, λ_2 and their spatial derivatives. The solution of equations of motion will be obtained for the biological membrane tube. This analysis, presented below would also be useful if a thin layer of fluid is assumed to exist between the shell and the sphere. It would be necessary in this case to solve the lubrication equations and shell equations respectively.

Let us consider an inertial cylindirical coordinate system i whose origin is located at the center of the sphere at time $t = 0$. Velocity of the fixed edge is zero and boundary A moves with speed V_0 with respect to this reference frame. Material points of the shell at boundary A will change continously with time t. Ley us denote the speed of these material points of the middle surface located instantaneously at A by V_1. Then a solution for the deformation of the

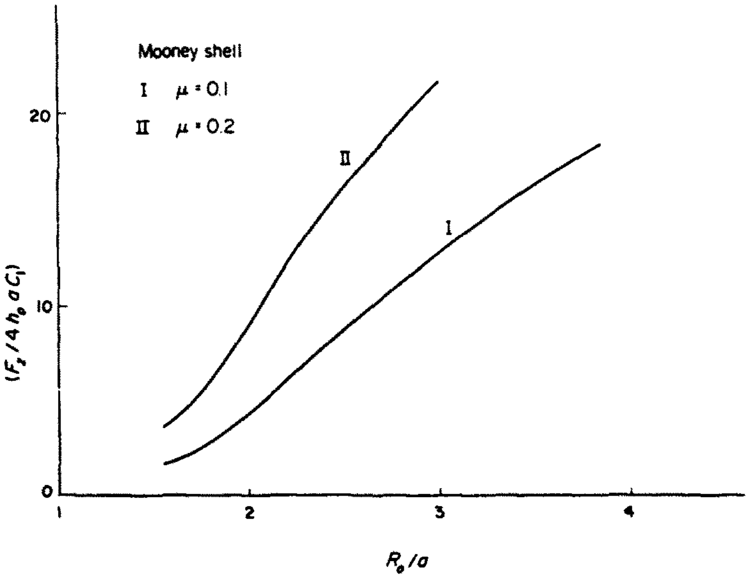

(a)

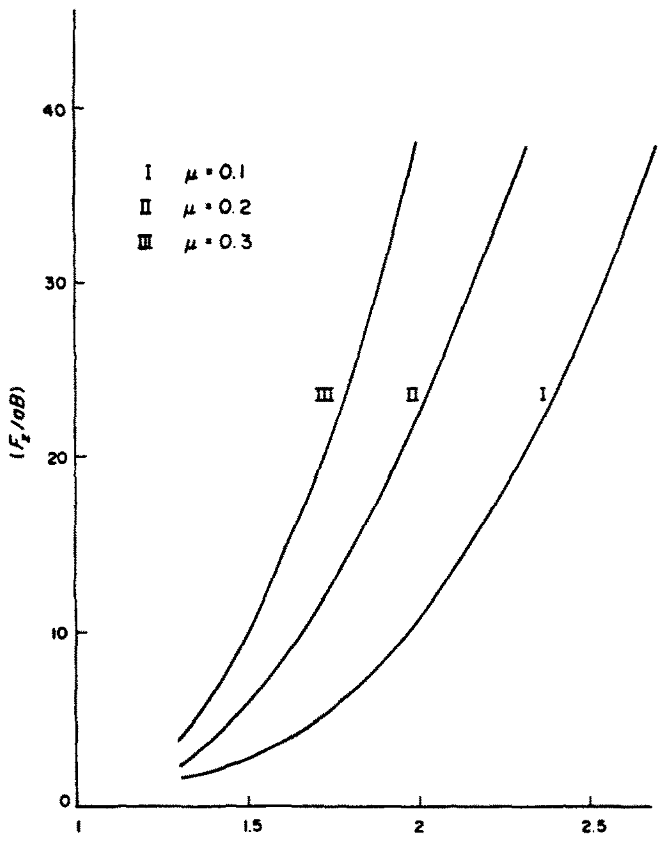

(b)

Fig. 8. Force required to pull the sphere with constant speed vs diameter ratio λ: (a) Mooney shell; (b) biological shell.

shell will be seeked in the form

$$r = r(\hat{s} \geqq (V_0 - V_1)t) \quad (49)$$

$$z = z(\hat{s} + (V_0 - V_1)t) + V_0 t \quad (50)$$

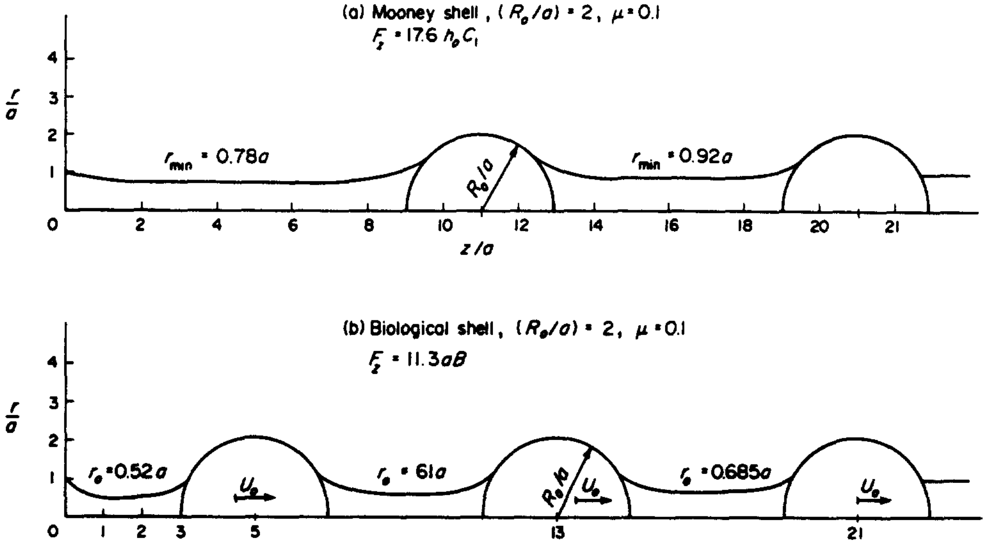

Fig. 9. Finite deformations of elastic shell caused by a line of spheres: (a) Mooney shell; (b) biological shell.

where $\mathring{S}$ is the arclength along the underformed meridian. At time $t = 0$, $\mathring{S} = 0$ for material points instantaneously at A and increases in the direction towards the fixed edge. It will be desired to express velocity and acceleration as a function of the arclength s, along the deformed meridian of the shell. Using the relations

$$\frac{dr}{d\mathring{s}} = \frac{dr}{ds}\frac{ds}{d\bar{s}}, \quad \lambda_1 = \frac{d\bar{s}}{d\bar{s}} \tag{51}$$

where $\bar{s} = (\mathring{s} + (V_0 - V_1)t)$, velocity and acceleration vectors on the middle surface can be written as

$$\mathbf{V} = V_0\mathbf{e}_z - (V_0 - V_1)\lambda_1\mathbf{e}_s \tag{52}$$

$$\mathbf{a} = \frac{(V_0 - V_1)^2}{a}[a\lambda_1\lambda_1,\, s\mathbf{e}_s + (a^2\lambda_1{}^2\lambda_2,\, ss/(1-(a\lambda_2,\, s)^2))^{1/2}\mathbf{e}_n] \tag{53}$$

where $\mathbf{e}_z$, $\mathbf{e}_s$, $\mathbf{e}_n$ are the unit vectors in axial, tangential and normal directions to the middle surface and $\lambda_1,\, s = d\lambda_1/ds$.

Bending stiffness of the shell will be neglected and the term $(d\lambda_2/ds)$ may be discontinous at the moving boundary A. In order to derive the conditions at this location, integrated form of the momentum equation is considered

$$\frac{\partial}{\partial t}\int_a^b \rho r \mathbf{V}\, d\mathring{s} = \boldsymbol{\phi}(b, t) - \boldsymbol{\phi}(a, t) + \mathbf{P} \tag{54}$$

where $\boldsymbol{\phi} = r(dz/ds)T_1\mathbf{e}_z$, $\mathbf{P}$ is the concentrated force per unit length along the azimuthal direction at the moving boundar $\mathring{s} = \sigma(t)$, and ρ is the areal density. The interval of integration, $a < \mathring{S} < b$ is chosen to contain $\mathring{s} = \sigma(t)$ at time t. Tensions T_1, T_2 are assumed to be continous and equal to zero at A. In the limit as a and b tend to $\mathring{S} = \sigma(t)$, this equation reduces to

$$\rho(V_0 - V_1)^2(\mathbf{e}_z + \mathbf{e}_s) = \mathbf{P}. \tag{55}$$

Hence, the resultant force acting on the moving sphere at location A becomes

$$\bar{\mathbf{P}} = 2\pi a \rho (V_0 - V_1)^2 \left(1 - \frac{1}{\lambda}\right) \mathbf{e}_z. \tag{56}$$

In order to find a relation between V_0 and V_1 conservation of mass equation will be considered. The part of the shell that lies in the domain $z_m < z < z_A$ will be chosen as the control volume. The subscript m denotes that section of the shell with $\lambda_2 = \lambda_{2m}$ and further away from the fixed edge. Noting that the shell material is incompressible, this eqn leads to the following relation

$$V_1 = V_0(1 - \lambda_{2m}\lambda_{3m}). \tag{57}$$

If there was no slip between the shell and the sphere, this equation shows that the motion described by eqns (49) and (50) would not be possible. Either the minimum radius, or the thickness of the shell would vanish as the sphere moves further away from the fixed edge.

Equation (57) was used to plot dimensionless relative velocity $(V_0 - V_1)/V_1$ against μ for $\lambda = 2$ in Fig. 10. Coefficient of friction μ, diameter ratio λ and speed V_0 are the three parameters that determine λ_{2m} and λ_{3m}. Solution of Section 4 was employed in calculating λ_{2m} and λ_{3m} which are not very sensitive to the value of V_0.

Equations of motion (3) and (4) including the inertial terms described above are solved for the biological membrane shell by using the computational scheme presented in Section 4.

In order to proceed with numerical integration, it was expendient to introduce the parameter G defined as

$$G = \rho(V_0 - V_1)^2/B \tag{58}$$

where B is the elasticity coefficient of the biological membrane. Knowing the speed V_0 of the particle is not sufficient to determine G (eqn 57). In order to combine the solutions at free boundary B for given values of V, (R_0/a) and μ, an initial value for λ_{2m} is selected to start the iterative procedure. For each new λ_{2m} value parameter G must be recalculated by using (57) and (58) and be inserted in solutions valid in the domains $(z_B < z < z_A)$ and $(z_m < z < z_B)$. Location of boundary B changes with increasing the value of V_0. Consideration of shell inertia shows that resultant axial force on a cross section normal to the z axis is not uniform when G is not equal to zero. This force has its maximum value at the fixed edge (Fig. 11). Hence the force F_z required to pull the sphere is smaller than the force F_z^W at the fixed edge. This is expected because the acceleration of particles on the midsurface of the shell remaining between the fixed edge and section B is towards the fixed edge. Figure 12 shows the variation of F_z and F_z^W as a

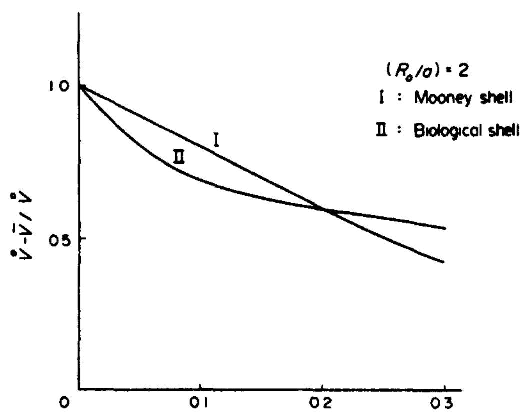

Fig. 10. Variation of dimensionless relative speed $(V_0 - V_1)/V_0$ vs coefficient of friction μ((I) Mooney shell; (II) biological shell).

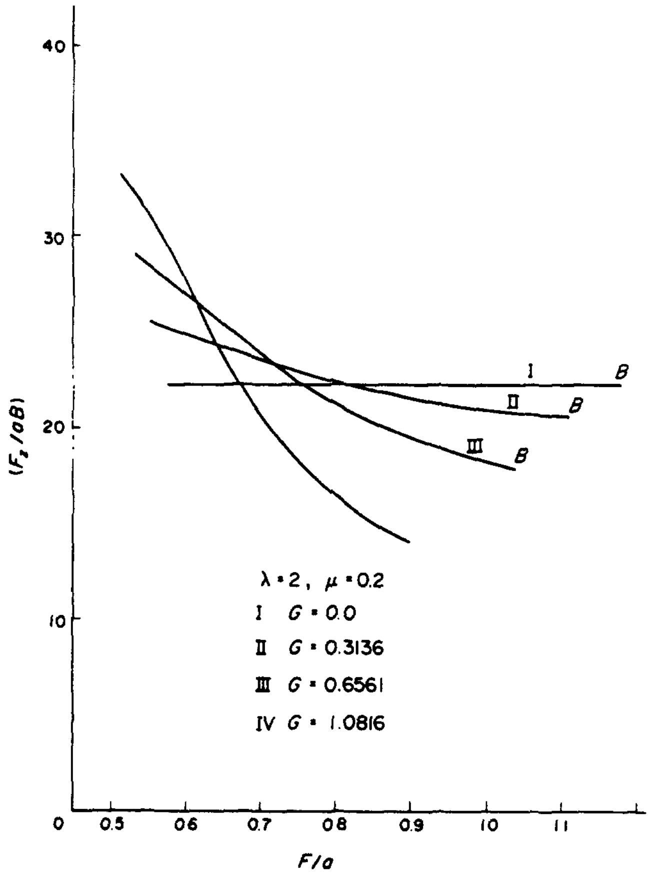

Fig. 11. Variation of resultant force on a cross section normal to the z axis vs dimensionless radial distance, (r/a).

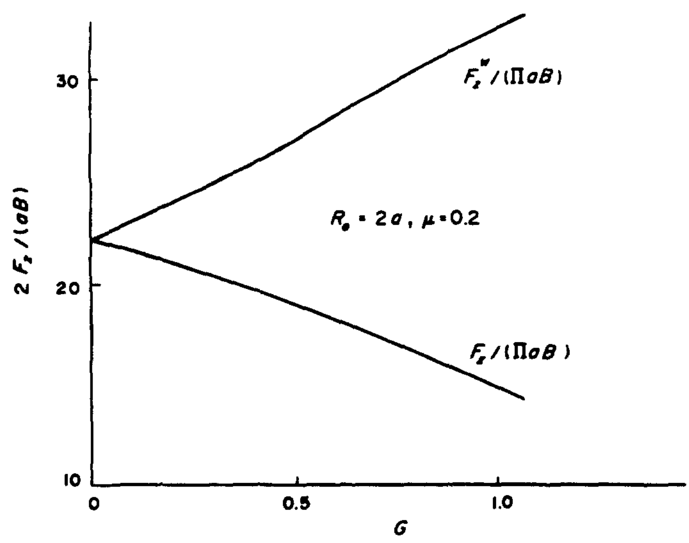

Fig. 12. Variation of the force F_z required to pull the sphere and F_z^W, the reaction force at the fixed edge vs shell inertia parameter.

function of parameter G for $\lambda = 2$ and $\mu = 0.2$. As the speed V_0 of the spherical particle increases the force F_z decreases. It is known that apparent viscosity η decreases with increasing speed V_0 of spherical elastic particles in a rigid tube filled with fluid [1]. However this is a mechanically different phenomen caused by the increase of the gap thickness between the sphere and the shell for larger V_0 values.

REFERENCES

1. H. Tözeren and R. Skalak, The steady flow of Closely fitting incompressible elastic spheres in a tube. *J. Fluid Mech.* **7**, 1–16 (1978).
2. P. R. Zarda, S. Chien and R. Skalak, Elastic deformation of red blood cells *J. Biomech.* **10**, 211–221 (1977).
3. C. C. Huang, Forced motions of elastic cylindrical shells. *J. Appl. Mech.* **46**, 321 (1975).
4. A. Ertepinar, Stability and vibrations of thick walled tubes subject to finite twist and external pressure. *Int. J. Solids Structures* **15**, 718 (1978).
5. R. Burridge and J. B. Keller, Peeling, slipping and cracking—some free boundary problems in mechanics *SIAM Rev.* **20**, 31–61 (1978).
6. S. Timoshenko and S. Woinowsky-Krieger, *Theory of Plates and Shells*, p. 434. McGraw-Hill, New York (1959).
7. H. D. Conway, Effects of friction on normal contact stresses *Trans ASME*, 1095–1096 (1971).
8. D. F. Moore, *The Friction and Lubrication of Elastomers*. Pergamon Press, Oxford (1972).
9. R. Skalak, A. Tözeren, R. P. Zarda and S. Chien, Strain energy function of red blood cell membranes *Biophysical J.* **13**, 926 (1973).
10. A. E. Green and A. Adkins, *Large Elastic Deformation*, 2nd Edn. Oxford University Press (1970).